Available online at www.sciencedirect.com
SCIENCE DIRECT®
Journal of Sound and Vibration 292 (2006) 402–414
JOURNAL OF SOUND AND VIBRATION
www.elsevier.com/locate/jsvi

Damping of flexural vibration using low-density, low-wave-speed media

Kripa K. Varanasi[1], Samir A. Nayfeh*

Department of Mechanical Engineering, Massachusetts Institute of Technology, Cambridge, MA 02139, USA

Received 8 September 2004; received in revised form 21 September 2005; accepted 16 October 2005
Available online 10 January 2006

Abstract

Significant damping of structural vibration can be attained by coupling to the structure a low-density medium (such as a powder or foam) in which the speed of sound propagation is relatively low. We describe a set of experiments in which flexural vibration of aluminum beams over a broad frequency range is damped by introduction of a layer of lossy low-wave-speed foam. At frequencies high enough to set up standing waves through the thickness of the foam, loss factors as high as 0.05 can be obtained with a foam layer whose mass is 3.9% of that of the beam. We model the foam as a continuum in which waves of dilatation and distortion can propagate, obtain approximate solutions for the frequency response of the system by means of a modal expansion, and find that the predictions are in close agreement with the measured responses. Finally, we develop a simple approximation for the system loss factor based on the complex wavenumber associated with flexural vibration in an infinite beam.
© 2005 Published by Elsevier Ltd.

1. Introduction

The introduction of a granular material or foam into a structure or machine is a relatively simple and low-cost approach to attenuation of vibration. Traditionally, dense granular fills (such as sand, lead shot, or steel balls) have been selected for such applications in order to obtain strong coupling between the structure and the granular material. Many researchers have studied the use of granular materials for vibration suppression. Panossian [1,2] carried out several experiments in which structures are filled with various types of particles (metallic, non-metallic, and even liquid particles) of various shapes and sizes at appropriate locations for attenuation of sound and vibration. Papalou and Masri [3,4] have developed an approximate method to predict the damping attained by dampers filled with steel balls of various sizes. Cremer and Heckl [5] suggested that a granular material such as sand can be modeled as a continuum, and that damping in a structure filled with such a granular material can be increased by adjusting dimensions so that standing waves occur in the granular material at the resonant frequencies of the structure.

*Corresponding author. Tel.: +1 617 253 2407; fax: +1 617 253 7549.
E-mail addresses: kripa@alum.mit.edu (K.K. Varanasi), nayfeh@alummit.edu (S.A. Nayfeh).
[1]Present address: GE Global Research, Niskayuna, NY.

0022-460X/$ - see front matter © 2005 Published by Elsevier Ltd.
doi:10.1016/j.jsv.2005.10.014

Richards and Lenzi [6] carried out several experiments on sand-filled tubes and have studied the influence of the quantity of sand, grain size, cavity shape and size, and the direction and amplitude of excitation. They report that damping attains a maximum at frequencies where resonances can be set up in the granular medium. Bourinet and Le Houedec [7] expanded on the ideas of Cremer and Heckl and developed a quantitative model for the vibration of beams filled with granular materials. They model compressive waves in the granular material in the direction transverse to the vibration to develop an "apparent mass", which they couple to a Timoshenko beam. However, these high-density fills add a great deal of mass to a structure and hence are rarely used where weight is a concern.

Experiments by Fricke [8] showed that a low-density granular fill can provide high damping of structural vibration over a broad range of frequencies. Varanasi [9] and Varanasi and Nayfeh [10] performed further experiments on beams with low-density granular fills and, by treating the fill as a compressible fluid in which dilatation waves can propagate, made quantitative predictions of the system response. They predicted that similar damping could be attained using any lossy medium (such as a foam) in which the speeds of wave propagation are low enough that waves can be set up in the medium at the frequencies of interest.

In this paper, we summarize a set of experiments on aluminum beams coupled to free and covered layers of a low-density foam. Then, modeling the foam as an isotropic continuum, we predict the response of the beam–foam systems based on a full modal expansion in terms of the mode shapes of the undamped beam. Finally, based on the complex wavenumber, we develop a simpler approximation for the loss factor associated with flexural vibration of such systems.

2. Experiments

We study beam–foam systems of the configuration shown in Fig. 1. An aluminum beam of rectangular cross section 38.1×12.7 mm is coupled to a 12.7 mm thick layer of EAR C-3201 [11] energy-absorbing foam using 3 M Contact 80 neoprene adhesive [12]. The density of the foam is $104.1\,\mathrm{kg/m^3}$ and, as detailed in the appendix, we determine that its Poisson's ratio ν is approximately 0.36 and its complex extensional modulus E is approximately $2075\omega^{1/2}(1+0.8\mathrm{j})$ Pa (for ω between 300 and 12 600 rad/s). Based on these measurements, we calculate the complex wave speeds in dilatation and shear at 1000 Hz to be $42.5(1+0.35\mathrm{j})\,\mathrm{m/s}$ and $25.7(1+0.35\mathrm{j})\,\mathrm{m/s}$, respectively.

In all of the experiments, the beams are suspended by soft elastic strings to simulate free–free boundary conditions. An impulsive excitation is provided by an impact hammer (PCB333A30 [13]) at one end of the beam, and the response is measured by an accelerometer (PCB353B11 [13]) located at the other end of the beam.

In Fig. 2, we plot the force-to-acceleration frequency response obtained for a beam of length 1448 mm with and without the foam layer. As expected, the beams without foam exhibit very little damping, with the loss factor $\eta < 0.0001$ for each of the modes. When a layer of foam of thickness 12.7 mm is glued to the beam, the increase in damping in the first four modes is very small, but there is a significant increase in that of the fifth and higher modes. Based on the speeds of sound in the foam, we find that the sixth mode occurs in a frequency

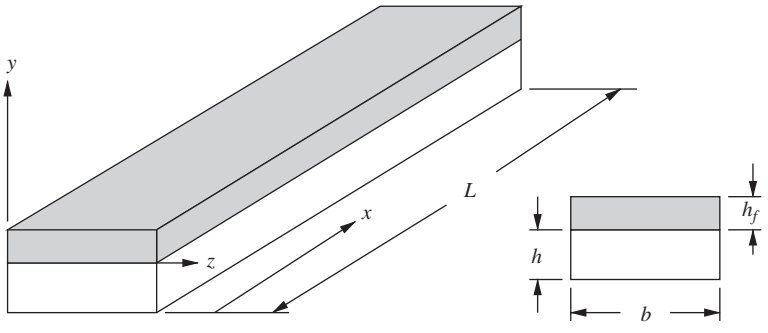

Fig. 1. Schematic of the beam–foam system.

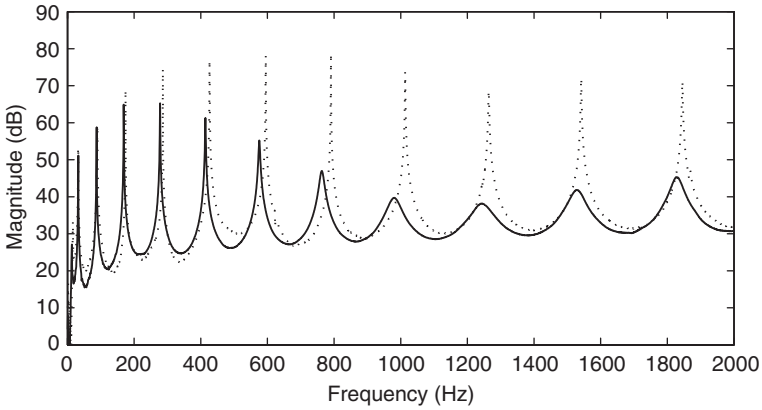

Fig. 2. Measured force-to-acceleration frequency responses for a beam of length 1448 mm under impact excitation: without foam (dotted) and with foam (solid).

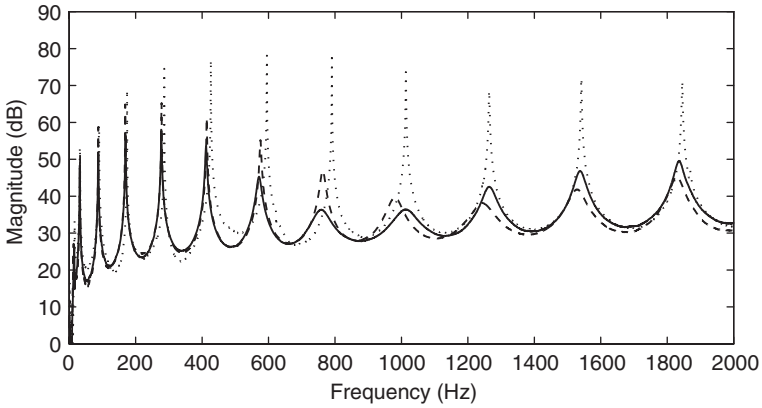

Fig. 3. Measured force-to-acceleration frequency responses under impact excitation: without foam (dotted), with foam (dashed), and with an auxiliary 0.05 mm thick steel layer (solid).

range where quarter-wavelength dilatation and half-wavelength shear waves can be set up through the thickness of the foam.

Next, in Figs. 3 and 4, we plot the force-to-acceleration frequency-response curves measured for sandwich beams formed by the addition of thin ''auxiliary'' metal layers atop the layer of foam. With the addition of the steel layers with thicknesses of 0.05 and 0.10 mm, the damping is increased in the fifth and higher modes. We find that the addition of these steel layers has resulted in a significant increase in damping at lower frequencies with a relatively small increase in mass (1.2% and 2.4% for the 0.05 and 0.10 mm thick steel layers, respectively).

3. Model

In this section, we develop a model by which the responses measured in Section 2 can be predicted. Consider a beam of length L to which is attached a layer of foam as shown in Fig. 1. The beam is excited by a point-harmonic force at a frequency ω and distance x_f from one end of the beam. We employ a simple Euler–Bernoulli model for the beam and consider the foam to be a lossy and isotropic continuum in which waves of dilatation and distortion can propagate.

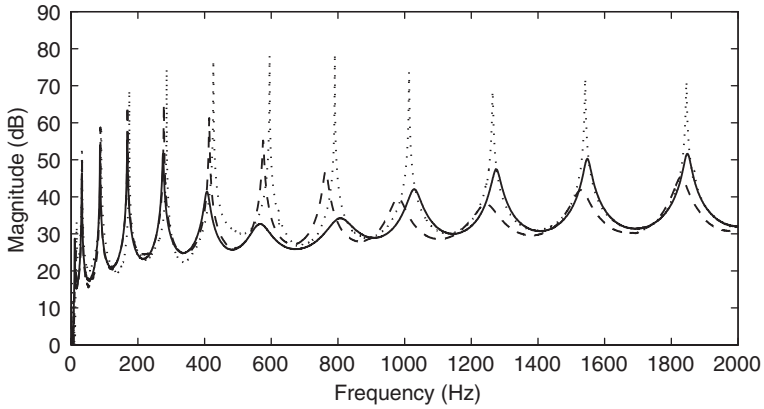

Fig. 4. Measured force-to-acceleration frequency responses under impact excitation: without foam (dotted), with foam (dashed), and with an auxiliary 0.10 mm thick steel layer (solid).

The foam used in the experiments described in Section 2 is an elastic-porous medium in which frame-borne and air-borne waves can propagate (e.g., Refs. [14,15]). The stress induced on the beam by the air-borne waves scales as the product of the bulk modulus of the air in the pores times the volumetric strain in air. Hence although these waves can have a significant influence on sound and noise transmission, we can safely neglect their effect on the vibration of the beam in comparison to the effect of the frame-borne waves. We therefore treat the foam as an isotropic continuum in which frame-borne waves of dilatation and distortion arising from the bulk properties of the material can propagate. We characterize the foam by a loss factor η, complex Young's modulus of elasticity $E = \hat{E}(1 + \mathrm{j}\eta_f \operatorname{sgn}\omega)$, and Poisson ratio v. We detail in the appendix a set of measurements carried out to determine these properties for the foam used in our experiments.

3.1. Equations of motion

Consider steady vibration of the beam–foam system of Fig. 1 under harmonic excitation at a frequency ω by a point force $\mathrm{Re}(F\delta(x - x_f)\mathrm{e}^{\mathrm{j}\omega t})$. We denote the vibratory deflection of the beam under such an excitation by $\mathrm{Re}(V(x,\omega)\mathrm{e}^{\mathrm{j}\omega t})$ and the displacements of the foam in the x and y directions by $\mathrm{Re}(u(x,y,\omega)\mathrm{e}^{\mathrm{j}\omega t})$ and $\mathrm{Re}(v(x,y,\omega)\mathrm{e}^{\mathrm{j}\omega t})$, respectively. The displacements $u(x,y,\omega)$ and $v(x,y,\omega)$ in the foam are governed by the second-order wave equations of a linear and isotropic continuum (e.g., Ref. [16])

$$(\lambda + 2G)u_{xx} + Gu_{yy} + (\lambda + G)v_{xy} + \rho\omega^2 u = 0, \tag{1}$$

$$Gv_{xx} + (\lambda + 2G)v_{yy} + (\lambda + G)u_{xy} + \rho\omega^2 v = 0, \tag{2}$$

where the subscripts denote partial differentiation and ρ, $\lambda = vE/(1 + v)(1 - 2v)$, and G are, respectively, the density, complex Lamé constant, and complex shear modulus of the foam.

At the interface of the beam and foam (that is, at $y = 0$), the normal stress $\sigma_y(x,0,\omega)$ in the foam contributes to a force in the y direction whereas the shear stress $\tau_{xy}(x,0,\omega)$ in the foam results in a moment about the neutral axis. We therefore write the equation governing the transverse deflection V of the beam in the form

$$D\frac{\partial^4 V}{\partial x^4} - m\omega^2 V - b\sigma_y(x,0,\omega) - \frac{bh}{2}\frac{\partial\tau_{xy}(x,0,\omega)}{\partial x} = F\delta(x - x_f), \tag{3}$$

where b and h are, respectively, the width and height of the beam's cross section, D is its flexural stiffness, and m is its mass per unit length.

3.2. Boundary conditions for the foam

At the interface between the foam and beam (at $y = 0$), the displacements in the foam must match those of the surface of the beam. Hence we write

$$v(x, 0, \omega) = V(x, \omega), \tag{4}$$

$$u(x, 0, \omega) = -\frac{h}{2}\frac{\partial V(x, \omega)}{\partial x}. \tag{5}$$

At the free surface of the foam (at $y = h_f$), the normal and shear stresses must vanish. Hence we have

$$\lambda u_x(x, h_f, \omega) + (\lambda + 2G)v_y(x, h_f, \omega) = 0, \tag{6}$$

$$u_y(x, h_f, \omega) + v_x(x, h_f, \omega) = 0. \tag{7}$$

Because the foam layers used in the experiments are long and slender, and strong damping is observed at frequencies at or above the frequencies at which the lengths of waves in the foam are on the order of the thickness of the foam, we do not enforce the boundary conditions on the ends of the foam (at $x = 0$ and L). This simplification allows us to reasonably approximate the behavior of the foam over most of the length of the beam and to obtain relatively simple predictions of the effect of the foam on the vibration of the beam.

3.3. Modal expansion

We seek solutions of the equations of motion (1)–(3) along with the boundary conditions (4)–(7). In this section, we compute the frequency response of the beam–foam system by expanding the deflection of the beam in terms of the mode shapes of an undamped beam, solving for compatible responses in the foam, and summing to obtain the forced response at each frequency.

We expand the deflection of the beam in terms of the eigenfunctions of an undamped beam as

$$V(x, \omega) = V_{01}(\omega) + V_{02}(\omega)(x - L/2) + \sum_{n=1}^{N} V_n(\omega)(\alpha_n(x) + \beta_n(x)). \tag{8}$$

The first two terms in this expansion represent pure translation and rotation of the beam. The remaining terms in the expansion are the flexible modes of the beam, where the $\alpha_n(x)$ and $\beta_n(x)$ denote, respectively, the propagating and evanescent components of the nth flexible mode of the beam. For the nth mode of a free–free beam, $\alpha_n(x)$ and $\beta_n(x)$ are given by

$$\alpha_n(x) = \sin(k_n x) + p_n \cos(k_n x), \tag{9}$$

$$\beta_n(x) = \sinh(k_n x) + p_n \cosh(k_n x), \tag{10}$$

where k_n is the wavenumber associated with the nth mode and p_n is a constant given by

$$p_n = \frac{\sin(k_n L) - \sinh(k_n L)}{\cosh(k_n L) - \cos(k_n L)}. \tag{11}$$

3.3.1. Contribution of beam flexible modes

Based on the form of the modal expansion (8) and boundary conditions (4) and (5), we take the displacements in the foam to be

$$v(x, y, \omega) = \sum_{n=1}^{N} \chi_n(y, \omega)\alpha_n(x) + \sum_{n=1}^{N} \xi_n(y, \omega)\beta_n(x), \tag{12}$$

$$u(x, y, \omega) = \sum_{n=1}^{N} \phi_n(y, \omega)\alpha_n'(x)/k_n + \sum_{n=1}^{N} \psi_n(y, \omega)\beta_n'(x)/k_n, \tag{13}$$

Table 1
Form of the coefficient matrix A_n in Eq. (14)

$$\begin{bmatrix}
0 & 1 & 0 & 0 & 0 & 0 & 0 & 0 \\
-\dfrac{\rho\omega^2 - k_n^2(\lambda+2G)}{G} & 0 & 0 & 0 & 0 & -\dfrac{\lambda+G}{G}k_n & 0 & 0 \\
0 & 0 & 0 & 1 & 0 & 0 & 0 & 0 \\
0 & 0 & -\dfrac{\rho\omega^2 + k_n^2(\lambda+2G)}{G} & 0 & 0 & 0 & 0 & -\dfrac{\lambda+G}{G}k_n \\
0 & 0 & 0 & 0 & 0 & 1 & 0 & 0 \\
0 & \dfrac{\lambda+G}{\lambda+2G}k_n & 0 & 0 & -\dfrac{\rho\omega^2 - k_n^2 G}{\lambda+2G} & 0 & 0 & 0 \\
0 & 0 & 0 & 0 & 0 & 0 & 0 & 1 \\
0 & 0 & 0 & -\dfrac{\lambda+G}{\lambda+2G}k_n & 0 & 0 & -\dfrac{\rho\omega^2 + k_n^2 G}{\lambda+2G} & 0
\end{bmatrix}$$

where the primes denote the first derivative and the χ_n, ξ_n, ϕ_n, and ψ_n are yet to be determined functions of y and ω. Substituting the above expansions for u and v into the wave equations (1) and (2), we obtain a system of ordinary differential equations that can be rearranged into the first-order form

$$X_n' = A_n X_n, \tag{14}$$

where the vector X_n is composed of

$$X_n = (\phi_n \quad \phi_n' \quad \psi_n \quad \psi_n' \quad \chi_n \quad \chi_n' \quad \xi_n \quad \xi_n')^{\mathrm{T}} \tag{15}$$

and the matrix A_n is given in Table 1.

Next, we solve Eq. (14) subject to the boundary conditions (4)–(7) to obtain

$$X_n = B_n \mathrm{e}^{\Lambda_n y} c_n V_n, \tag{16}$$

where the B_n and Λ_n are, respectively, the matrices of eigenvectors and eigenvalues obtained by diagonalizing the A_n, and the c_n are constant vectors whose elements are determined by enforcing the boundary conditions (4)–(7). Thus, having obtained the functions χ_n, ξ_n, ϕ_n, ψ_n and in terms of the V_n, we compute the stresses $\sigma_y(x,0)$ and $\tau_{xy}(x,0)$ at the interface of the foam. These, along with the expansion (8), are then substituted into Eq. (3) governing the beam deflection. A Galerkin projection onto the beam mode shapes yields a system of linear algebraic equations in the V_n whose order is equal to the number of terms in the expansion.

3.3.2. Contribution of beam rigid-body modes

When the beam undergoes pure translational motion, the displacement u in the x direction is zero everywhere in the foam. As a result, plane waves are excited in the y direction and the wave equations (1)–(2) reduce to the following simple form:

$$(\lambda + 2G)v_{yy} + \rho\omega^2 v = 0. \tag{17}$$

This equation is solved subject to the boundary conditions (4)–(7) to obtain the displacement $v(y,\omega)$ in the foam, and thence the normal stress exerted by the foam on the beam and the corresponding response $V_{01}(\omega)$ of the beam.

When the beam undergoes a rotational motion as described by the second term in Eq. (8), the boundary conditions on the foam require that the displacement u in the x direction in the foam be constant at the foam–beam interface and the displacement v in the y direction be linear in x at the interface of the foam and the beam. We therefore take the displacements in the foam to be of the form

$$v(x,y,\omega) = (x - L/2)\chi_0(y,\omega), \tag{18}$$

$$u(x,y,\omega) = \phi_0(y,\omega). \tag{19}$$

Substituting these displacements into the wave equations (1)–(2), we obtain differential equations for χ_0 and ϕ_0 in the form

$$(\lambda + 2G)\chi_0'' + \rho\omega^2\chi_0 = 0, \tag{20}$$

$$G\phi_0'' + (\lambda + 2G)\chi_0' + \rho\omega^2\phi_0 = 0. \tag{21}$$

Imposing the boundary conditions (4)–(7), we solve for the displacements in the foam and stresses exerted by the foam on the beam and then obtain the coefficient $V_{02}(\omega)$ in the expansion (8).

3.3.3. The total response

After computing the contributions to the displacement of the beam from the flexible and rigid-body modes, we write the non-dimensional accelerance R at the location of the sensor x_s as

$$R = \frac{m\omega^2 VL}{F} = \left(\frac{m\omega^2 L}{F}\right)\left(V_{01} + V_{02}(x_s - L/2) + \sum_{n=1}^{N} V_n[\alpha_n(x_s) + \beta_n(x_s)]\right). \tag{22}$$

Finally, we plot in Fig. 5 the computed force-to-acceleration frequency response and compare it with the measured response. We find that there is good agreement between the measured and predicted frequency responses. For each resonance, we extract the resonant frequency and loss factor from the measurements as well as the computed frequency responses using the modal curve-fitting software Star Modal [17] and compare their values in Table 2.

3.4. Sandwich beam

In this section, we develop a model for the sandwich beam formed by coupling an auxiliary layer to the foam–beam system discussed in the previous section. The auxiliary layer at $y = h_f$ changes the boundary conditions on the foam given by Eqs. (6) and (7). In the sandwich beam, we require at $y = h_f$ that the displacements $v(x, h_f, \omega)$ and $u(x, h_f, \omega)$ in the foam match those in the auxiliary layer. Hence, we have

$$v(x, h_f, \omega) = W(x, \omega), \tag{23}$$

$$u(x, h_f, \omega) = \frac{h_a}{2}\frac{\partial W(x, \omega)}{\partial x}, \tag{24}$$

where $\mathrm{Re}(W(x, \omega)e^{j\omega t})$ and h_a are, respectively, the deflection and thickness of the auxiliary beam. Taking into account the normal stress $\sigma_y(x, h_f)$ and shear stress $\tau_{xy}(x, h_f)$ in the foam, we write the equation governing the deflection W of the auxiliary beam in the form

$$D_a\frac{d^4W}{dx^4} - m_a\omega^2 W + b\sigma_y(x, h_f, \omega) - \frac{bh_a}{2}\frac{\partial\tau_{xy}(x, h_f, \omega)}{\partial x} = 0, \tag{25}$$

where D_a and m_a are, respectively, the flexural stiffness and the mass per unit length of the auxiliary beam.

To obtain the force-to-acceleration frequency response for the sandwich beam, we must simultaneously solve the wave equations (1)–(2) and the beam-deflection equations (3) and (25) subject to the boundary conditions (6), (7), (23), and (24). As in Section 3.3, we expand the deflection of the principal beam according to Eq. (8) and the deflection W of the auxiliary beam as

$$W(x, \omega) = W_{01}(\omega) + W_{02}(\omega)(x - L/2) + \sum_{n=1}^{N} W_n(\omega)(\alpha_n(x) + \beta_n(x)). \tag{26}$$

Compatible displacements in the foam are then written as in Eqs. (12) and (13) for the flexible modes, and as described in Section 3.3.2 for the rigid-body modes.

As in the case of the free foam layer, we determine the response in the foam corresponding to the nth beam mode by solving Eq. (14), but in this case use the boundary conditions (6), (7), (23), and (24). We obtain an

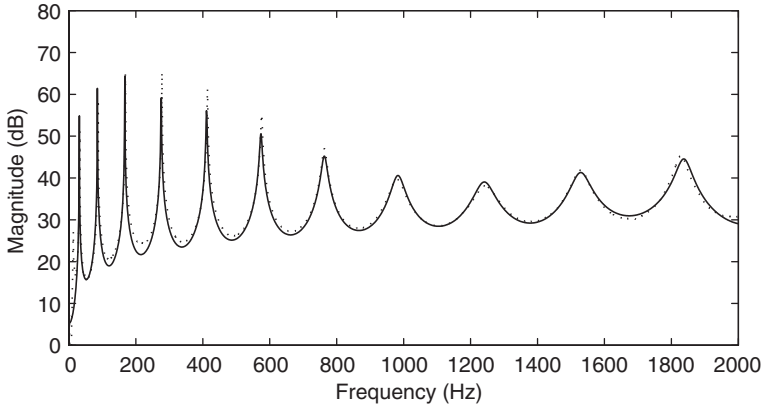

Fig. 5. Comparison of measured and predicted force-to-acceleration frequency responses for the beam with a free foam layer: measured (dotted) and predicted (solid).

Table 2
Comparison of measured and predicted modal loss factors for the beam with a free foam layer: the measurement and curve-fitting process for the loss factor yields results repeatable to ±5%

Frequency (Hz)	Loss factor	
	Measured	Predicted
32.4	0.0002	0.0001
87.7	0.0010	0.0002
169.0	0.0010	0.0010
277.9	0.0018	0.0020
413.9	0.0034	0.0048
575.7	0.0080	0.0100
763.1	0.0180	0.0208
979.9	0.0424	0.0400
1240.0	0.0522	0.0480
1530.0	0.0322	0.0348
1830.0	0.0206	0.0236

expression of the form

$$X_n = B_n e^{\Lambda_n y}(c_n V_n + d_n W_n), \tag{27}$$

where the B_n and Λ_n are, respectively, the matrices of eigenvectors and eigenvalues obtained by diagonalizing the A_n, and the c_n and d_n are constant vectors whose elements are determined by enforcing the boundary conditions (6), (7), (23), and (24). Based on this solution, we compute the stresses σ_y and τ_{xy} and substitute them into Eqs. (3) and (25) and project in turn onto the beam modes to obtain a set of linear equations in the V_n and W_n. Finally, we solve this system of equations to determine the coefficients V_n and W_n in the expansions (8) and (26). As before, the accelerance R at the sensor location is computed based on the V_n according to Eq. (22). The force-to-acceleration frequency responses thus obtained are in good agreement with the measured responses. They are plotted in Figs. 6 and 7.

4. Complex wavenumber approximation

The frequency responses based on full modal expansions agree closely with the experiments, but are cumbersome for design or quick calculation. In this section, we compute the complex wavenumber associated

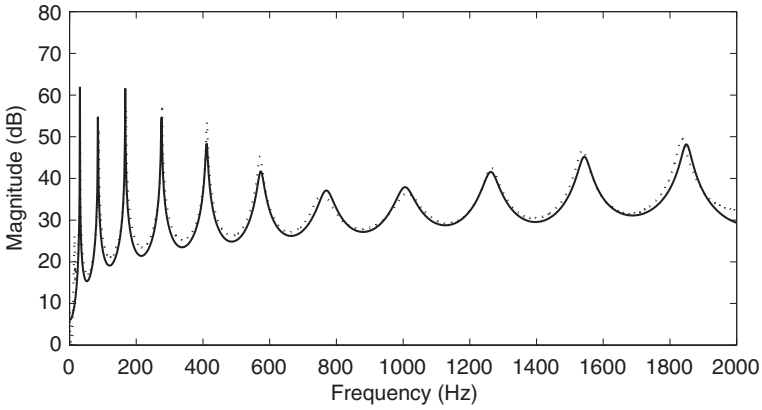

Fig. 6. Comparison of the measured and predicted force-to-acceleration frequency responses for a sandwich beam with a 0.05 mm steel auxiliary layer: measured (dotted), predicted (solid).

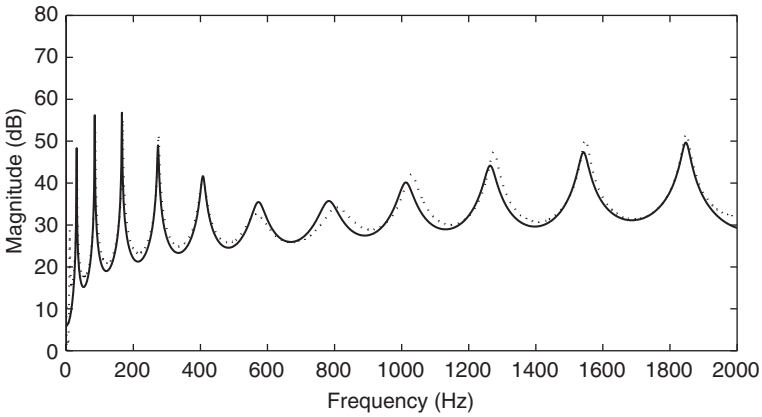

Fig. 7. Comparison of the measured and predicted force-to-acceleration frequency responses for a sandwich beam with a 0.10 mm steel auxiliary layer: measured (dotted), predicted (solid).

with harmonic motion of an infinitely long beam–foam system, and thence obtain a simpler estimate of the system loss factor.

Consider again the beam–foam system sketched in Fig. 1, but extending from $x = -\infty$ to $+\infty$. We write the steady harmonic bending deflection $V(x, \omega)$ of the beam in terms of decaying right and left traveling waves as

$$V(x,\omega) = V_+(\omega)\mathrm{e}^{-\mathrm{j}k_b x} + V_-(\omega)\mathrm{e}^{\mathrm{j}k_b x} \tag{28}$$

and seek solutions for the complex wavenumber k_b. Once k_b has been computed for a given frequency ω, the loss factor can be computed from

$$\eta = \frac{\mathrm{Im}(1/k_b^4)}{\mathrm{Re}(1/k_b^4)}. \tag{29}$$

Examining the form of the boundary conditions (4) and (5), we assume displacements in the foam in the y and x directions, respectively, in the form

$$v(x,y,\omega) = [V_+(\omega)\mathrm{e}^{-\mathrm{j}k_b x} + V_-(\omega)\mathrm{e}^{\mathrm{j}k_b x}]\psi(y/h_f), \tag{30}$$

$$u(x,y,\omega) = -\mathrm{j}[V_+(\omega)\mathrm{e}^{-\mathrm{j}k_b x} - V_-(\omega)\mathrm{e}^{\mathrm{j}k_b x}]\phi(y/h_f), \tag{31}$$

where ψ and ϕ are yet-to-be-determined functions of the dimensionless coordinate y/h_f through the thickness of the foam. Substituting the preceding forms into Eqs. (1) and (2) governing wave propagation in the foam, we obtain coupled second-order ordinary differential equations for ψ and ϕ in the form

$$\psi'' = \frac{h_f k_b}{2(1-\nu)}\phi' + \left[\left(\frac{1-2\nu}{2(1-\nu)}\right)(h_f k_b)^2 - \frac{(\omega h_f/c)^2}{1+\mathrm{j}\eta_f}\right]\psi, \tag{32}$$

$$\phi'' = -\frac{h_f k_b}{1-2\nu}\psi' + \left[(h_f k_b)^2 - \frac{(\omega h_f/c)^2}{1+\mathrm{j}\eta_f}\right]\left(\frac{2(1-\nu)}{1-2\nu}\right)\phi, \tag{33}$$

where the primes denote differentiation, we have made use of $\lambda = 2\nu G/(1-2\nu)$, and $c^2(1+\mathrm{j}\eta_f)$ is the square of the complex speed of propagation of plane compression waves in the foam given by

$$c^2(1+\mathrm{j}\eta_f) = \left(\frac{\lambda+2G}{\rho}\right). \tag{34}$$

In terms of ϕ and ψ, the boundary conditions on the foam given by Eqs. (4)–(7) become

$$\phi(0) = -\frac{hk_b}{2}, \quad \psi(0) = 1, \quad \psi'(1) = \frac{\nu h_f k_b \phi(1)}{1-\nu}, \quad \text{and} \quad \phi'(1) = -h_f k_b \psi(1) \tag{35}$$

and the dispersion relation (3) for the beam coupled to a layer of foam becomes

$$Dk_b^4 - m\omega^2 - b\left[(\lambda - G)\frac{hk_b^2}{2} + \frac{\lambda+2G}{h_f}\psi'(0) - \frac{Ghk_b}{2h_f}\phi'(0)\right] = 0. \tag{36}$$

We seek a solution for k_b that satisfies simultaneously this dispersion relation as well as the differential equations (32) and (33) and boundary conditions (35) governing wave propagation in the foam.

We obtain an iterative solution for k_b by first taking $k_b^4 = m\omega^2/D$; substituting this value into Eqs. (32), (33), and (35); and solving for the response in the foam. An improved estimate $\tilde{k}_b$ is then obtained from Eq. (36) according to

$$D\tilde{k}_b^{\,4} = m\omega^2 + b\left[(\lambda - G)\frac{hk_b^2}{2} + \frac{\lambda+2G}{h_f}\psi'(0) - \frac{Ghk_b}{2h_f}\phi'(0)\right] \tag{37}$$

and in turn substituted into Eqs. (32), (33), and (35) to solve for the response in the foam. The process is repeated until the estimates converge. For parameter values comparable to those in our experiments (where the mass of the foam is much smaller than the mass of the beam), the first estimate of the loss factor is quite good, usually within a few parts per thousand of its final value.

Therefore, a reasonable estimate of the loss factor can be made by substitution of the first iterate obtained from Eq. (37) directly into the expression (29) for the loss factor:

$$\eta \approx \frac{b\,\mathrm{Im}[(\bar{\lambda}-\bar{G})k_b^2 h/2 + (\bar{\lambda}+2\bar{G})\bar{\psi}'(0)/h_f - \bar{G}\bar{\phi}'(0)k_b h/2h_f]}{m\omega^2 + b\,\mathrm{Re}[(\bar{\lambda}-\bar{G})k_b^2 h/2 + (\bar{\lambda}+2\bar{G})\bar{\psi}'(0)/h_f - \bar{G}\bar{\phi}'(0)k_b h/2h_f]}. \tag{38}$$

The second term in the denominator is negligible in comparison with the first, which represents the inertia of the beam. We therefore make the further approximation that

$$\eta \approx \frac{\rho b h_f}{m}\left(\frac{c}{\omega h_f}\right)^2 \mathrm{Im}\left[(1+\mathrm{j}\eta_f)\left(\frac{4\nu-1}{4(1-\nu)}k_b^2 h h_f + \bar{\psi}'(0) - \frac{1-2\nu}{4(1-\nu)}k_b h\bar{\phi}'(0)\right)\right], \tag{39}$$

where $k_b^4 = m\omega^2/D$. Thus, according to this approximation, the loss factor of the system scales directly with $\rho b h_f/m$, the ratio of the mass of the foam to the mass of the beam. The dependence on the dimensionless frequency $\omega h_f/c$ is somewhat more complicated because it appears in the equations governing ϕ and ψ. The dimensionless parameter $h_f k_b$ (which is 2π times the ratio of the thickness of the foam to the length of flexural waves in the beam) also depends on frequency.

Consider again the experiment with the free foam layer, whose response is compared to that predicted by the full expansion in Fig. 5 and Table 2. The loss factors (normalized by mass ratio $\rho b h_f/m$) obtained from the

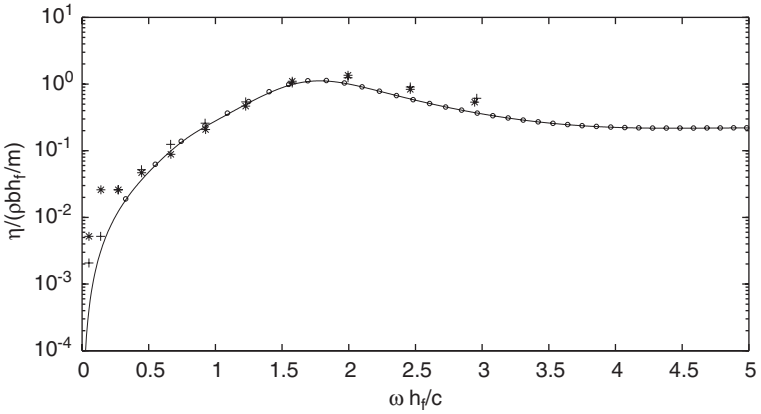

Fig. 8. Normalized loss factor $\eta/(\rho b h_f/m)$ for the beam with a free layer of foam as a function of dimensionless frequency $\omega h_f/c$: measurements (asterisks) and full expansion (plus signs) from Table 2, complex wavenumber approximations by iteration (solid line) and from Eq. (39) without iteration (circles).

experiment and full expansion are plotted as asterisks and plus signs, respectively, in Fig. 8. The estimate for the loss factor obtained by iteration on Eqs. (32), (33), (35), and (37) is plotted as a solid line, and that obtained without iteration from Eq. (39) is plotted as a series of circles. The various approximations are in good agreement with the experiments.

5. Conclusions

Significant damping can be attained with little added mass by coupling to a structure a lossy medium with low density and low speeds of wave propagation. At frequencies high enough to favor wave propagation through the thickness of the low-wave-speed medium, strong interactions occur between it and the vibrating structure, resulting in considerable damping. Such damping treatments (whether the low-density medium is powder, foam, or some other material) offer a low-cost method of attaining broad band damping in structures and machines with little creep, and has been applied to longitudinal and flexural vibration in belt-drives, compliant mechanisms, and precision structures [9].

For higher-order flexural, extensional, or torsional modes of a structure coupled to a low-wave-speed medium, good estimates of the damping over a given frequency range can be obtained by estimating the complex-wavenumber associated with wave propagation. For lower-order modes, the mode shape of the structure and its coupling to the medium must be taken into account.

Appendix. Material properties of the foam

In this section, we document a set of experiments conducted to determine the complex elastic moduli of the foam. The extensional and shear moduli are determined by exciting thin layers of foam sandwiched between aluminum blocks as shown in Fig. 9. We impose on the samples a harmonic displacement provided by an electromagnetic shaker and measure the force transmitted by the foam to obtain the acceleration-to-force frequency responses plotted in Fig. 10.

Noting that the magnitude of the response $M(\omega)$ has no resonance peaks and the phase $\theta(\omega)$ is more or less constant, we conclude that for the range of frequencies used in these experiments, wave propagation in the foam is negligible. We therefore treat it as a simple hysteretic spring (e.g., Refs. [18,19]) and compute its complex extensional modulus $\hat{E}(\omega)(1+\mathrm{j}\eta_f(\omega))$ from

$$\hat{E}(\omega)(1+\mathrm{j}\eta_f(\omega)) = \frac{\omega^2 M(\omega)(1-\mathrm{j}\tan\theta(\omega))}{\sqrt{1+(\tan\theta(\omega))^2}}\frac{t}{A}, \tag{40}$$

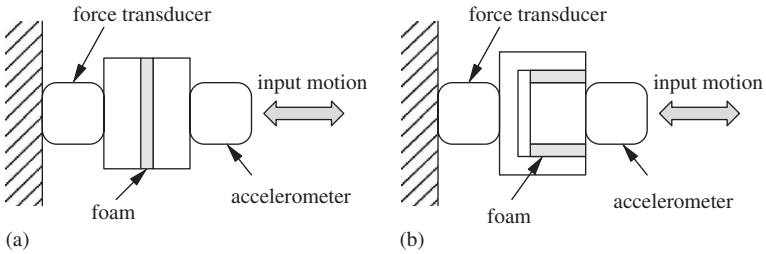

Fig. 9. Schematic of the experiment employed to determine (a) the extensional modulus and (b) the shear modulus of the foam.

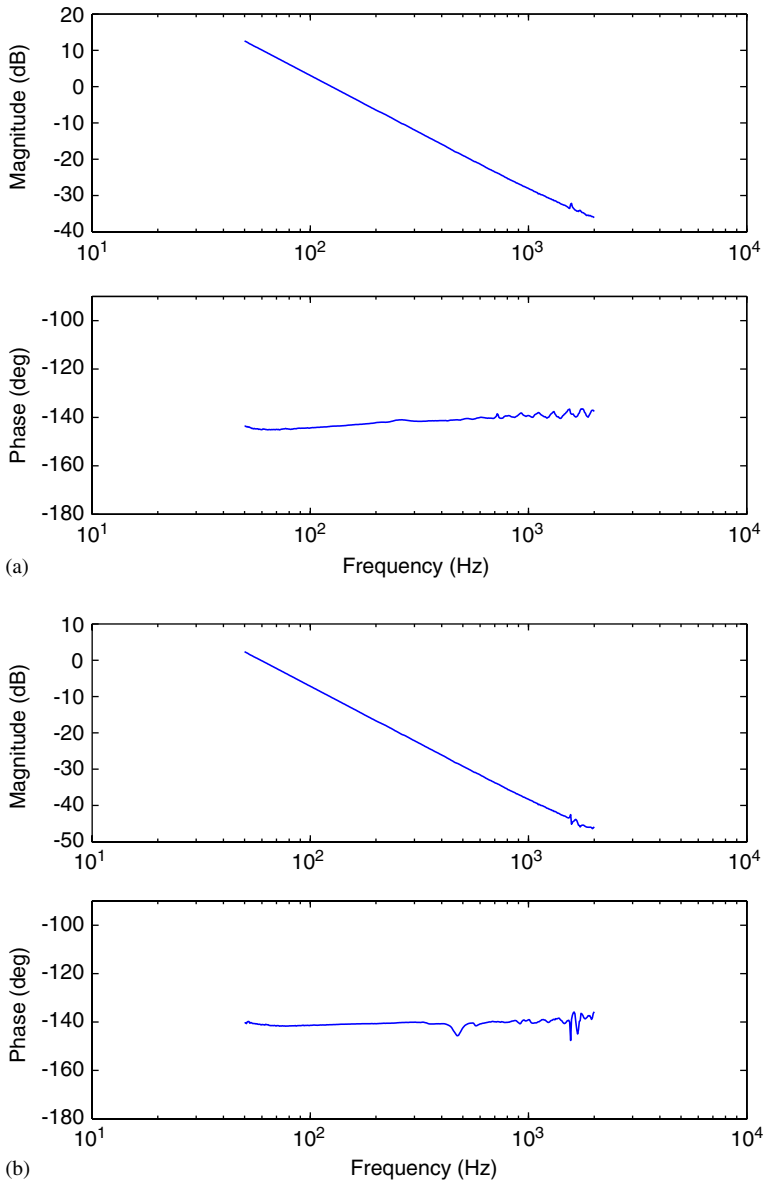

Fig. 10. Measured acceleration-to-force frequency response of the systems shown in Figs. 9(a) and (b), respectively.

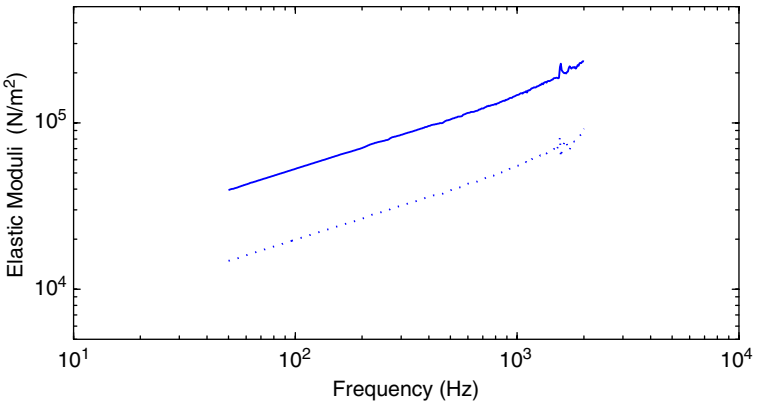

Fig. 11. Measured real part of the elastic moduli of foam: extensional modulus Re(E) (solid), shear modulus Re(G) (dotted).

where t and A are, respectively, the thickness and the cross-sectional area of the layer of foam. In Fig. 11, we plot the real part of the modulus E as a function of frequency and find that the extensional modulus is proportional to the square root of frequency. Because the phase of the acceleration-to-force transfer function is approximately -140° over the measured range of frequencies we estimate the loss factor of the foam in extension to be approximately 0.8. Carrying out a similar calculation, we determine the complex shear modulus and plot the result as a dotted line in Fig. 11. The ratio of the extensional and shear moduli is nearly constant over this range of frequencies, and the Poisson's ratio is approximately 0.36.

References

[1] H.V. Panossian, Structural damping enhancement via non-obstructive particle damping technique, *Journal of Vibration and Acoustics* 114 (1) (1992) 101–105.
[2] H.V. Panossian, Non-obstructive particle damping experience and capabilities, in: *Proceedings of IMAC–XX: A Conference on Structural Dynamics*, Vol. 4753, Los Angeles, CA, February 2002, SPIE, pp. 936–941.
[3] A. Papalou, S. Masri, Response of impact dampers with granular materials under random excitation, *Earthquake Engineering and Structural Dynamics* 25 (1996) 2530–2567.
[4] A. Papalou, S. Masri, An experimental investigation of particle dampers under harmonic excitation, *Journal of Vibration and Control* 4 (1998) 361–379.
[5] L. Cremer, M. Heckl, *Structure-Borne Sound*, Springer, Berlin, 1973.
[6] E.J. Richards, A. Lenzi, On the prediction of impact noise, VII: the structural damping of machinery, *Journal of Sound and Vibration* 97 (4) (1984) 549–586.
[7] J.M. Bourinet, D. Le Houedec, A dynamic stiffness analysis of damped tubes filled with granular material, *Computers & Structures* 73 (1999) 395–406.
[8] J.R. Fricke, Lodengraf damping—an advanced vibration damping technology, Journal of *Sound and Vibration* 34 (7) (2000) 22–27.
[9] K.K. Varanasi, *Vibration Damping using Low-Wave-Speed Media with Applications to Precision Machines*, Ph.D. Thesis, MIT, Cambridge, MA, 2004.
[10] K.K. Varanasi, S.A. Nayfeh, Damping of flexural vibration using low-density foams and granular materials, in: *DETC03*, *ASME Design Engineering Technical Conferences*, September 2003.
[11] E-A-R Speciality Composites, 7911 Zionsville Road, Indianapolis, IN 46268, EAR Technical Data Sheet.
[12] 3M Adhesives, St. Paul, MN 55144, Adhesive Data Sheet.
[13] PCB Piezotronics, 3425 Walden Avenue, Depew NY 14043, Shock and Vibration Sensors Catalog.
[14] M.A. Biot, Theory of propagation of elastic waves in a fluid-saturated porous solid, I: low-frequency range, II: higher frequency range, *Journal of the Acoustical Society of America* 28 (1956) 168–191.
[15] J.S. Bolton, N.M. Shiau, Y.J. Kang, Sound transmission through multi-panel structures lined with elastic porous materials, *Journal of Sound and Vibration* 191 (3) (1996) 22–27.
[16] S.P. Timoshenko, J.N. Goodier, *Theory of Elasticity*, third ed., McGraw-Hill, New York, 1970.
[17] Spectral Dynamics, Inc., 1010 Timothy Dr., San Jose, CA 95133, The STAR System Reference Manual.
[18] S.H. Crandall, The hysteretic damping model in vibration theory, *Journal of Mechanical Engineering Science* 25 (1991) 23–28.
[19] A.D. Nashif, D.I.G. Jones, J.P. Henderson, *Vibration Damping*, Wiley, New York, 1985.